

# The study of optical properties of $\text{In}_2\text{O}_3$ and of mixed oxides $\text{In}_2\text{O}_3\text{--MoO}_3$ system deposited by coevaporation

M. ANWAR\*

*Physics Department, Government College, Burewala, Pakistan*  
E-mail: dranwar03@brain.net.pk

I. M. GHOURI

*Centre for Advanced Studies in Physics, G. C. University, Lahore, Pakistan*

S. A. SIDDIQI

*Centre for Solid State Physics, University of the Punjab, Lahore, Pakistan*

Published online: 17 March 2006

A discussion of the optical properties of two systems of dielectric films i.e.  $\text{In}_2\text{O}_3$  and of mixed oxides  $\text{In}_2\text{O}_3\text{--MoO}_3$  system is presented. Film thickness, substrate temperature, annealing and composition (in molar%) have a profound effect on the structure and optical properties of these films. The decrease in optical band gap with the increase in film thickness of  $\text{In}_2\text{O}_3$  is interpreted in terms of incorporation of oxygen vacancies in the  $\text{In}_2\text{O}_3$  lattice. The decrease in optical band gap with the increase in substrate temperature and annealing of  $\text{In}_2\text{O}_3$  thin films is ascribed to the release of trapped electrons by thermal energy or by the outward diffusion of the oxygen-ion vacancies, which are quite mobile even at low temperature. For the mixed oxides  $\text{In}_2\text{O}_3\text{--MoO}_3$  system the results are found to be compatible with the reduction in the value of optical band gap of these materials as the molar fraction of  $\text{MoO}_3$  increases in the  $\text{In}_2\text{O}_3$  thin films and is attributed to the incorporation of Mo(VI) ions in an  $\text{In}_2\text{O}_3$  lattice that causes the indium orbital to become a little less tightly bound. The decrease in optical band gap of mixed oxides  $\text{In}_2\text{O}_3\text{--MoO}_3$  system, with increasing film thickness is interpreted in terms of incorporation of oxygen vacancies in both  $\text{In}_2\text{O}_3$  and  $\text{MoO}_3$  lattice which are also believed to be the source of conduction electrons in  $\text{In}_2\text{O}_3\text{--MoO}_3$  complex. The decrease in optical band gap with increasing substrate temperature and annealing of mixed oxides  $\text{In}_2\text{O}_3\text{--MoO}_3$  system is due to the increasing concentration of oxygen vacancies, formation of indium and molybdenum species of lower oxidation state and indium interstitials. The blue colouration of mixed oxides  $\text{In}_2\text{O}_3\text{--MoO}_3$  samples is due to the inter-electron transfer from oxygen 2p to molybdenum 4d level due to which Mo species of lower oxidation states are formed.

© 2006 Springer Science + Business Media, Inc.

## 1. Introduction

The technology of thin films has developed as a consequence of the wide use of thin dielectric films in microelectronic devices. Thin films used in microelectronic circuits and in research are primarily fabricated by thermal evaporation, electron beam evaporation, sputtering and by chemical processes [1]. Since the properties of thin films depend strongly on structure, stoichiometry and nature of the impurities present, it is in-

evitable that each deposition technique with its associated controlling parameters should yield films with different characteristics.

Although partial transparency, with acceptable reduction in conductivity, can be obtained for very thin metallic films, high transparency and simultaneously high conductivity cannot be obtained in intrinsic stoichiometric materials. It is well known that non-stoichiometric thin films exhibit high transmittance and nearly metallic

\*Author to whom all correspondence should be addressed.

conductivity. This can be achieved by creating electron degeneracy in a wide band gap material by controllably introducing non-stoichiometry. The degeneracy is caused by oxygen vacancies created during film deposition [2].

The group III compound semiconductors are becoming important in a number of technological applications.  $\text{In}_2\text{O}_3$  is an oxide having fairly high electrical conductivity and some times used for transparent electrodes. Ohta *et al.* [3] have shown the presence of indium interstitial at remarkably high concentration. Its high conduction electrons concentrations are believed to result from the interstitial indium atoms [4, 5] or oxygen vacancies [6, 7] in the  $\text{In}_2\text{O}_3$  structure.

$\text{In}_2\text{O}_3$  is an n-type semiconducting material and its observed optical transparency arises from the relatively wide direct band gap. Several researchers [8–10] have published surveys on various aspects of  $\text{In}_2\text{O}_3$  in order to understand the energy band structure, which for amorphous thin films of  $\text{In}_2\text{O}_3$ , may be considerably different from that of a single crystal because of their sub-stoichiometric composition and possible long-range order.

Thin films of indium oxide are used as transparent conductors in many electro-optical devices. Optically transparent electrically conducting films of  $\text{In}_2\text{O}_3$  are useful in a variety of applications. To develop highly sensitive gas sensor, various kinds of n-type semiconductors made of  $\text{In}_2\text{O}_3$  have been prepared.

Relatively less information about  $\text{MoO}_3$  films is available in the literature because of the considerable difficulties in preparing specimen suitable for investigation of physical properties. However several researchers [11–15] have published survey on various aspects of  $\text{MoO}_3$ . Kharrazi *et al.* [16] have reported that the optical absorption is associated with the electrons trapped by negative ion vacancies, which thereby form colour centres.

Ivanova *et al.* [17] and Zhao *et al.* [18] have studied the surface properties of stoichiometric and oxygen deficient crystalline  $\text{MoO}_3$  and reported that heating in vacuum induced some reduction of the  $\text{MoO}_3$  surface whereby Mo(VI) ions were reduced to Mo(V) and there is diffusion between the surface region and bulk.

Siokou *et al.* [19] and Yahya *et al.* [20] have studied the electronic structure of crystalline molybdenum oxide by photoelectron study and reported that blue coloured  $\text{MoO}_3$  samples contain trapped electrons at oxygen vacancies. Madhuri *et al.* [21] have also observed the same phenomenon.

The study of the optical properties of evaporated thin films of mixed oxides  $\text{In}_2\text{O}_3$ – $\text{MoO}_3$  system prepared by co-evaporation technique will help to elucidate the basic properties of these oxides. Particular attention has been given to the question of substrate temperature during deposition and also subsequent annealing, since these conditions are known to have a profound effect on the structure, composition and optical properties of films. A comprehensive comparison of the optical properties of  $\text{In}_2\text{O}_3$  and of mixed oxides system  $\text{In}_2\text{O}_3$ – $\text{MoO}_3$  is carried out and results are discussed in terms of current theory.

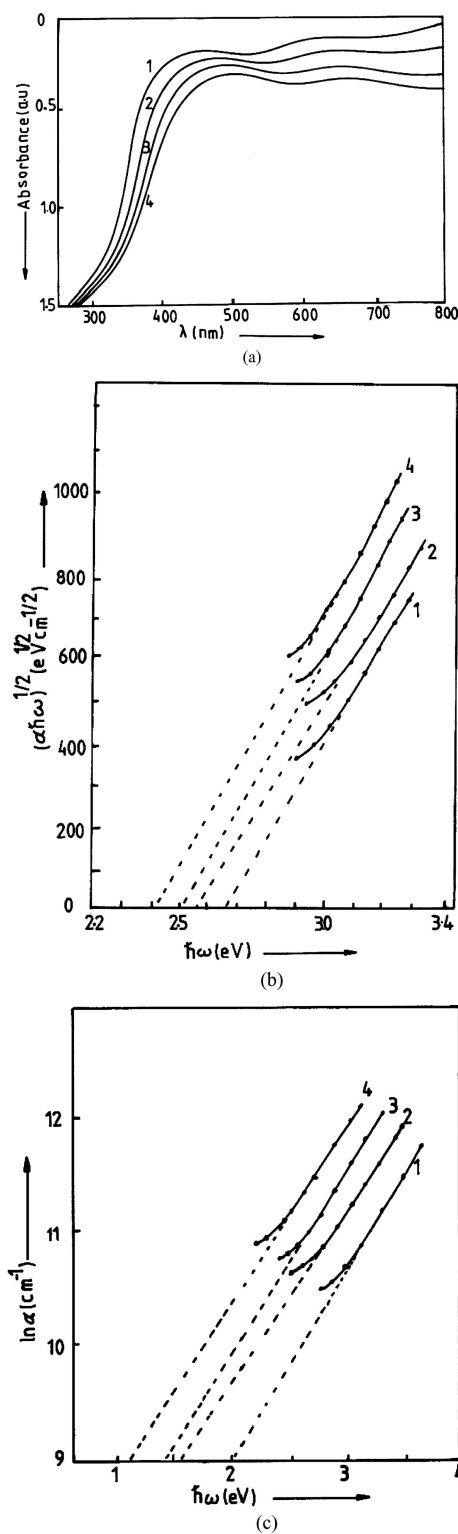


Figure 1 (a) Optical absorption spectra of amorphous thin films of  $\text{In}_2\text{O}_3$  as a function of wavelength, deposited at  $20^\circ\text{C}$ , for different thicknesses, (1) 100 nm, (2) 200 nm, (3) 300 nm, (4) 400 nm. (b) The plot of  $(\alpha\hbar\omega)^{1/2}$  versus  $(\hbar\omega)$ , using the data of (a), of amorphous thin films of  $\text{In}_2\text{O}_3$ , deposited at  $20^\circ\text{C}$ , for different thicknesses, (1) 100 nm, (2) 200 nm, (3) 300 nm, (4) 400 nm. (c) The plot of  $\ln(\alpha)$  versus  $(\hbar\omega)$ , using the data of (a), of amorphous thin films of  $\text{In}_2\text{O}_3$ , deposited at  $20^\circ\text{C}$ , for different thicknesses, (1) 100 nm, (2) 200 nm, (3) 300 nm, (4) 400 nm.

## 2. Experimental work

Thin evaporated layers of  $\text{In}_2\text{O}_3$  and of mixed oxides  $\text{In}_2\text{O}_3\text{-MoO}_3$  system were prepared in a Balzers BA510 coating unit on clean corning 7059 glass substrate held at a pressure of about  $1.33 \times 10^{-4}$  Pa. Molybdenum boats were used for evaporation of both  $\text{In}_2\text{O}_3$  and  $\text{MoO}_3$ . An Edwards quartz crystal monitor, monitored the evaporation rates and finally the film thickness was measured by using an M-100 Angstrometer, which operates on the principle of multiple beam interferometry. Varying the evaporation rates of the component oxides could change the molar composition of the constituent oxide layer in a mixed oxide film. For any two oxides A and B, the thickness and molar percentage in the mixed film are related as follows,

$$\frac{A(\text{mol}\%)}{B(\text{mol}\%)} = \frac{\text{Thickness of A} \times \text{density of A/mol. wt. of A}}{\text{Thickness of B} \times \text{density of B/mol. wt. of B}}$$

A number of films were deposited and only those films were selected for absorption measurements whose thicknesses were in exact numbers such as 100, 200, 300 nm etc. All other techniques used for cleaning the glass substrate, raising the substrate temperature, absorption measurements, transmission electron microscopy and annealing the samples in vacuum are the same as described earlier by Anwar *et al.* [22].

The plots of absorbance A versus wavelength for amorphous thin films of  $\text{In}_2\text{O}_3$  and of mixed oxides  $\text{In}_2\text{O}_3\text{-MoO}_3$  system were obtained with a Perkin-Elmer Lambda 9 spectrometer in the wavelength range 250–850 nm using slit width of 2 nm and a medium speed scan.

The films of  $\text{MoO}_3$  and of mixed oxides (75 mol%  $\text{In}_2\text{O}_3\text{-25 mol.}\% \text{MoO}_3$ ). deposited at room temperature showed no evidence of colour. As the temperature of the substrates was increased, the colour of the films changed initially to light blue and then to dark blue at higher substrate temperature.

## 3. Results

The optical properties of evaporated amorphous thin films of  $\text{In}_2\text{O}_3$  have been studied as a function of film thickness, substrate deposition temperature and annealing. The optical absorption spectra of amorphous thin layers of  $\text{In}_2\text{O}_3$  have been studied in the thickness range 100–400 nm deposited on the substrates kept at  $20^\circ\text{C}$  (Fig. 1a). Some samples of constant thickness  $\approx 300$  nm have been studied in the substrate deposition temperature range  $20\text{--}270^\circ\text{C}$  (Fig. 2a). A few samples of constant thickness  $\approx 300$  nm, deposited at  $20^\circ\text{C}$ , were annealed in vacuum for 4 h in the temperature range  $200\text{--}500^\circ\text{C}$ . The optical absorption spectra for the samples were recorded immediately after the films were cooled to room temperature (Fig. 3a).

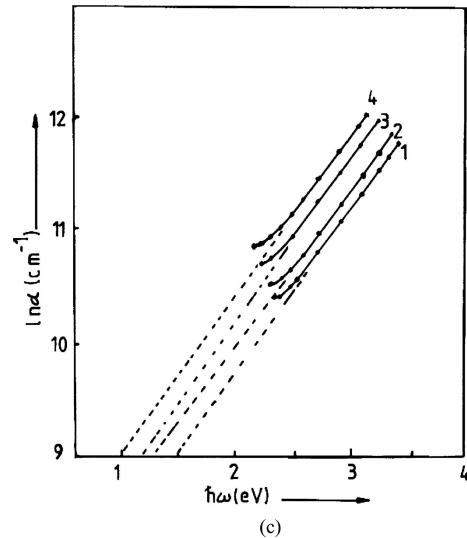
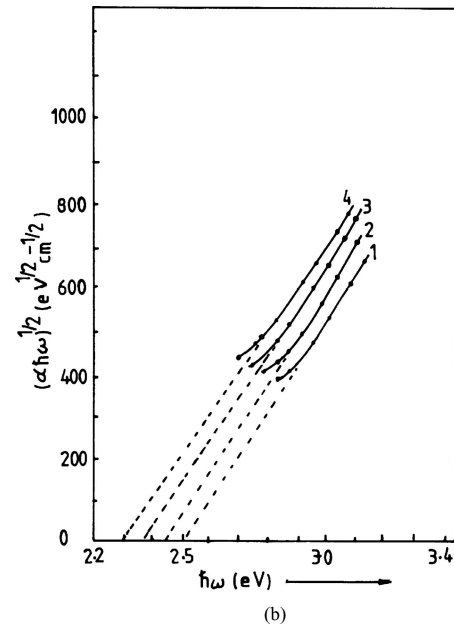
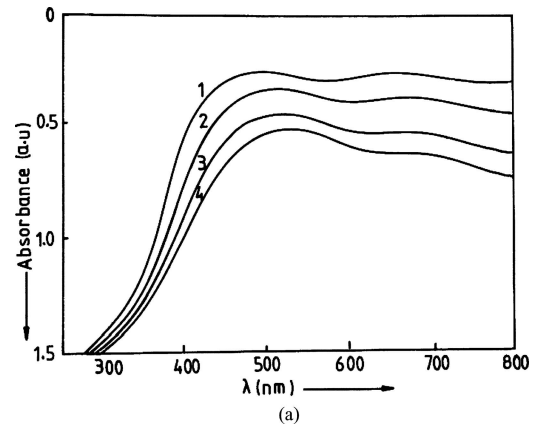


Figure 2 (a) Optical absorption spectra of 300 nm thick amorphous thin films of  $\text{In}_2\text{O}_3$  as a function of wavelength, for different substrate temperatures, (1)  $20^\circ\text{C}$ , (2)  $100^\circ\text{C}$ , (3)  $200^\circ\text{C}$ , (4)  $270^\circ\text{C}$ . (b) The plot of  $(\alpha\hbar\omega)^{1/2}$  versus  $(\hbar\omega)$ , using the data of (a), of amorphous thin films of  $\text{In}_2\text{O}_3$ , for different substrate temperatures, (1)  $20^\circ\text{C}$ , (2)  $100^\circ\text{C}$ , (3)  $200^\circ\text{C}$ , (4)  $270^\circ\text{C}$ . (c) The plot of  $\ln(\alpha)$  versus  $(\hbar\omega)$ , using the data of (a), of amorphous thin films of  $\text{In}_2\text{O}_3$ , for different substrate temperatures, (1)  $20^\circ\text{C}$ , (2)  $100^\circ\text{C}$ , (3)  $200^\circ\text{C}$ , (4)  $270^\circ\text{C}$ .

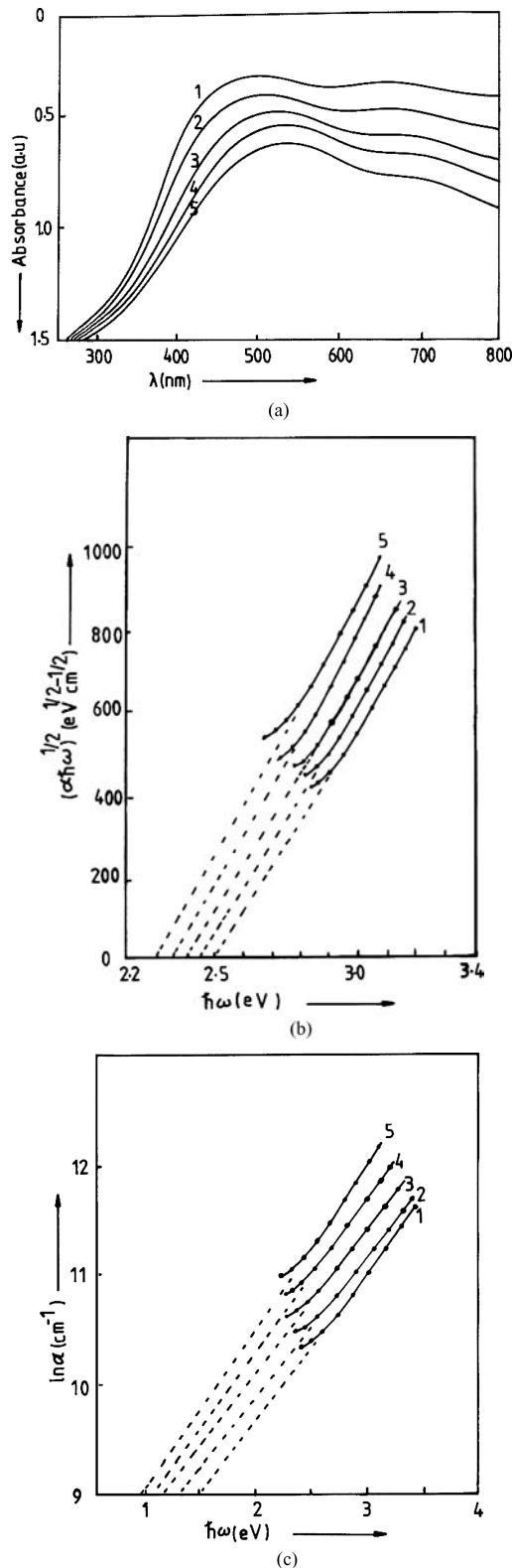


Figure 3 (a) Optical absorption spectra of 300 nm thick amorphous thin films of  $\text{In}_2\text{O}_3$  as a function of wavelength, deposited at  $20^\circ\text{C}$ , for different annealing temperatures, (1) as evaporated, (2)  $200^\circ\text{C}$ , (3)  $300^\circ\text{C}$ , (4)  $400^\circ\text{C}$ , (5)  $500^\circ\text{C}$ . (b) The plot of  $(\alpha\hbar\omega)^{1/2}$  versus  $(\hbar\omega)$ , using the data of (a), of amorphous thin films of  $\text{In}_2\text{O}_3$ , deposited at  $20^\circ\text{C}$ , for different annealing temperatures, (1) as evaporated, (2)  $200^\circ\text{C}$ , (3)  $300^\circ\text{C}$ , (4)  $400^\circ\text{C}$ , (5)  $500^\circ\text{C}$ . (c) The plot of  $\ln(\alpha)$  versus  $(\hbar\omega)$ , using the data of (a), of amorphous thin films of  $\text{In}_2\text{O}_3$ , deposited at  $20^\circ\text{C}$ , for different annealing temperatures, (1) as evaporated, (2)  $200^\circ\text{C}$ , (3)  $300^\circ\text{C}$ , (4)  $400^\circ\text{C}$ , (5)  $500^\circ\text{C}$ .

The optical absorption spectra of amorphous thin layers of mixed oxides  $\text{In}_2\text{O}_3\text{-MoO}_3$  system of constant thickness  $\approx 300$  nm keeping the substrates at  $20^\circ\text{C}$  during deposition have been studied with different compositions (in molar%) (Fig. 4a) Some samples were studied at fixed composition (85 mol.%  $\text{In}_2\text{O}_3\text{-15 mol.% MoO}_3$ ) deposited on the substrates kept at  $20^\circ\text{C}$ , having thickness in the range 100–400 nm (plot not shown in the text). Further samples of fixed composition (85 mol.%  $\text{In}_2\text{O}_3\text{-15 mol.% MoO}_3$ ) having constant thickness  $\approx 300$  nm, have been studied in the substrate deposition temperature range  $20\text{--}270^\circ\text{C}$  (plot not shown in the text). A few samples of fixed composition (85 mol.%  $\text{In}_2\text{O}_3\text{-15 mol.% MoO}_3$ ) having constant thickness  $\approx 300$  nm and deposited at  $20^\circ\text{C}$ , have been annealed in vacuum for 4 h in the temperature range  $200\text{--}500^\circ\text{C}$ . The optical absorption spectra for the mixed oxides  $\text{In}_2\text{O}_3\text{-MoO}_3$  thin films have been recorded immediately after the films were cooled to room temperature (plot not shown in the text).

It has been observed that the absorption edges moved towards higher wavelength region with increase in film thickness, substrate deposition temperature and annealing the thin films of both  $\text{In}_2\text{O}_3$  and of mixed oxides  $\text{In}_2\text{O}_3\text{-MoO}_3$  system. The absorption coefficient  $\alpha$  was determined, near the absorption edge, at different photon energies for all samples by using the relation;

$$\alpha = \frac{2.303A}{d} \quad (1)$$

where  $d$  is the thickness of the film and  $A$  is the absorbance, which is given by the relation  $(\log I_0/I_t)$ , where  $I_0$  and  $I_t$  are the intensities of incident and transmitted beams. In the high absorption region, where  $\alpha \geq 10^4$  cm<sup>-1</sup>, the absorption coefficient  $\alpha$  obeys the following relation [23, 24].

$$\alpha = \frac{B(\hbar\omega - E_{\text{opt}})^n}{\hbar\omega} \quad (2)$$

where  $\hbar\omega$  is the energy of the incident photon,  $E_{\text{opt}}$  is the optical band gap energy,  $n$  is an index which may have values 2, 3, 1/2, 3/2 depending upon the nature of the interband electronic transitions [25] and  $B$  is a constant which can be defined as

$$B = \frac{4\pi\sigma_o}{n_r c E_e} \quad (3)$$

where  $c$  is the velocity of light,  $\sigma_o$  is the value of conductivity extrapolated to  $1/T = 0$ ,  $E_e$  is the width of the tail of localized states in the band gap and  $n_r$  is the refractive index of the material. Equation 2 with  $n = 2$  has been successfully applied to many amorphous thin oxide films [21–25] and suggests absorption by non-direct transition with fairly constant matrix elements and a relaxed  $k$ -conservation selection rules. The

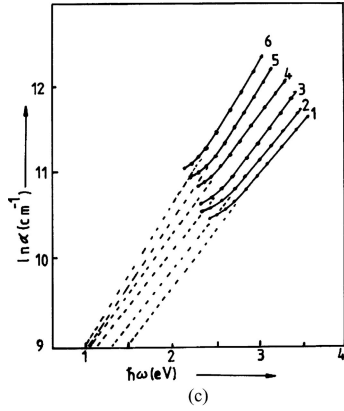
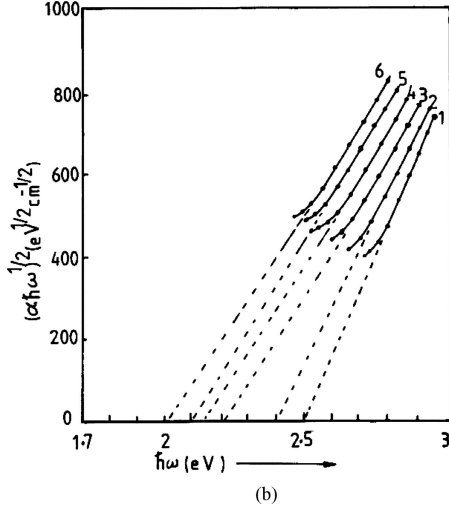
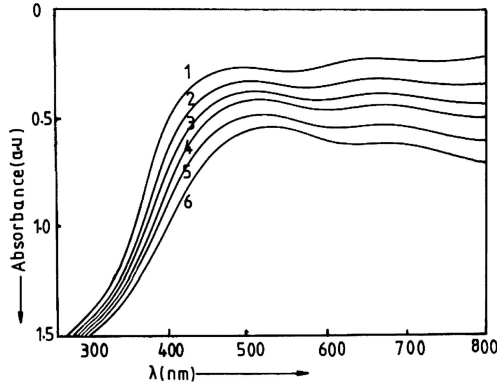


Figure 4 (a) Optical absorption spectra of 300 nm thick amorphous thin films of mixed oxides  $\text{In}_2\text{O}_3\text{-MoO}_3$  as a function of wavelength, deposited at  $20^\circ\text{C}$ , for different compositions (in molar%), (1) (100%  $\text{In}_2\text{O}_3$ ), (2) (95 mol.%  $\text{In}_2\text{O}_3\text{-5 mol.% MoO}_3$ ), (3) (90 mol.%  $\text{In}_2\text{O}_3\text{-10 mol.% MoO}_3$ ), (4) (85 mol.%  $\text{In}_2\text{O}_3\text{-15 mol.% MoO}_3$ ), (5) (80 mol.%  $\text{In}_2\text{O}_3\text{-20 mol.% MoO}_3$ ), (6) (75 mol.%  $\text{In}_2\text{O}_3\text{-25 mol.% MoO}_3$ ). (b) The plot of  $(\alpha\hbar\omega)^{1/2}$  versus  $(\hbar\omega)$ , using the data of (a), of 300 nm thick amorphous thin films of mixed oxides  $\text{In}_2\text{O}_3\text{-MoO}_3$ , deposited at  $20^\circ\text{C}$ , for different compositions (in molar%), (1) (100%  $\text{In}_2\text{O}_3$ ), (2) (95 mol.%  $\text{In}_2\text{O}_3\text{-5 mol.% MoO}_3$ ), (3) (90 mol.%  $\text{In}_2\text{O}_3\text{-10 mol.% MoO}_3$ ), (4) (85 mol.%  $\text{In}_2\text{O}_3\text{-15 mol.% MoO}_3$ ), (5) (80 mol.%  $\text{In}_2\text{O}_3\text{-20 mol.% MoO}_3$ ), (6) (75 mol.%  $\text{In}_2\text{O}_3\text{-25 mol.% MoO}_3$ ). (c) The plot of  $\ln(\alpha)$  versus  $(\hbar\omega)$ , using the data of (a), of 300 nm amorphous thin films of mixed oxides  $\text{In}_2\text{O}_3\text{-MoO}_3$ , deposited at  $20^\circ\text{C}$ , for different compositions (in molar%), (1) (100%  $\text{In}_2\text{O}_3$ ), (2) (95 mol.%  $\text{In}_2\text{O}_3\text{-5 mol.% MoO}_3$ ), (3) (90 mol.%  $\text{In}_2\text{O}_3\text{-10 mol.% MoO}_3$ ), (4) (85 mol.%  $\text{In}_2\text{O}_3\text{-15 mol.% MoO}_3$ ), (5) (80 mol.%  $\text{In}_2\text{O}_3\text{-20 mol.% MoO}_3$ ), (6) (75 mol.%  $\text{In}_2\text{O}_3\text{-25 mol.% MoO}_3$ ).

TABLE I Effect of film thickness on some optical parameters of amorphous  $\text{In}_2\text{O}_3$  thin films, deposited on the substrates at  $20^\circ\text{C}$

Film thickness (nm)	$E_{\text{opt}}$ (eV)	$E_e$ (eV)
100	2.65	0.70
200	2.55	0.76
300	2.50	0.82
400	2.40	0.90

TABLE II Effect of substrate deposition temperature on some optical parameters of amorphous  $\text{In}_2\text{O}_3$  thin films of constant thickness  $\approx 300$  nm

Substrate deposition temperatures ( $^\circ\text{C}$ )	$E_{\text{opt}}$ (eV)	$E_e$ (eV)
20	2.50	0.82
100	2.44	0.88
200	2.38	0.92
270	2.30	1.00

TABLE III Effect of annealing temperature on some optical parameters of amorphous  $\text{In}_2\text{O}_3$  thin films of constant thickness  $\approx 300$  nm, deposited at  $20^\circ\text{C}$

Annealing temperature ( $^\circ\text{C}$ )	$E_{\text{opt}}$ (eV)	$E_e$ (eV)
As evaporated	2.50	0.82
200	2.46	0.86
300	2.40	0.90
400	2.35	0.95
500	2.30	1.00

results obtained from absorption spectra were plotted as  $(\alpha\hbar\omega)^{1/2}$  versus photon energy  $(\hbar\omega)$  to find the value of  $E_{\text{opt}}$ . It can be seen that there exists a linear dependence of  $(\alpha\hbar\omega)^{1/2}$  with the photon energy  $(\hbar\omega)$  except at low photon energies where a band tailing comes into picture. This suggests that at high photon energies ( $\alpha \geq 10^4 \text{ cm}^{-1}$ ) the transition occurring in the present films is of indirect type. The values of optical band gaps are obtained by extrapolating the linear region of the lines to meet  $(\hbar\omega)$  axis at  $(\alpha\hbar\omega)^{1/2} = 0$ . The plots of  $(\alpha\hbar\omega)^{1/2}$  as a function of photon energy  $(\hbar\omega)$  are obtained from the data of Figs 1a–4a and are shown in Figs 1b–4b. The values of  $E_{\text{opt}}$  are estimated and listed in the Tables I–IV. The plots of  $(\alpha\hbar\omega)^{1/2}$  versus  $(\hbar\omega)$  for film thickness, substrate temperature and annealing of mixed oxides  $\text{In}_2\text{O}_3\text{-MoO}_3$  system are not shown in the text, but for comparison the values of  $E_{\text{opt}}$  are estimated and listed in the Tables V–VII. For absorption coefficient  $\alpha(\omega) \leq 10^4 \text{ cm}^{-1}$  there is usually an Urbach [26] tail in which  $\alpha$  depends exponentially on photon energy  $\hbar\omega$  as:

$$\alpha(\omega) = \alpha_0 \exp \frac{\hbar\omega}{E_e} \quad (4)$$

where  $\alpha_0$  is a constant,  $\omega$  is the angular frequency of the radiation and  $E_e$  is an energy, which is constant or

TABLE IV Effect of change in composition (in mol.%) on some optical parameters of amorphous  $\text{In}_2\text{O}_3$ - $\text{MoO}_3$  thin films of thickness  $\approx 300$  nm deposited at  $20^\circ\text{C}$

Film composition (mol.%)	$E_{\text{opt}}$ (eV)	$E_c$ (eV)
100 $\text{In}_2\text{O}_3$	2.50	0.82
95 $\text{In}_2\text{O}_3$ -5 $\text{MoO}_3$	2.42	0.87
90 $\text{In}_2\text{O}_3$ -10 $\text{MoO}_3$	2.22	0.91
85 $\text{In}_2\text{O}_3$ -15 $\text{MoO}_3$	2.15	0.95
80 $\text{In}_2\text{O}_3$ -20 $\text{MoO}_3$	2.10	0.97
75 $\text{In}_2\text{O}_3$ -25 $\text{MoO}_3$	2.00	1.00

TABLE V Effect of film thickness on some optical parameters of amorphous thin films of fixed composition (85 mol.%  $\text{In}_2\text{O}_3$ -15 mol.%  $\text{MoO}_3$ ) deposited at  $20^\circ\text{C}$

Sample thickness (nm)	$E_{\text{opt}}$ (eV)	$E_c$ (eV)
100	2.25	0.90
200	2.20	0.92
300	2.15	0.95
400	2.09	0.98

TABLE VI Effect of substrate deposition temperature on some optical parameters of amorphous thin films of fixed composition (85 mol.%  $\text{In}_2\text{O}_3$ -15 mol.%  $\text{MoO}_3$ ) having thickness  $\approx 300$  nm

Substrate deposition temperatures ( $^\circ\text{C}$ )	$E_{\text{opt}}$ (eV)	$E_c$ (eV)
20	2.15	0.95
100	1.82	0.98
200	1.62	1.05
270	1.42	1.10

weakly temperature-dependent and is often interpreted as the width of the tail of localized states in the band gap. In low energy region ( $\alpha(\omega) \leq 10^4 \text{ cm}^{-1}$ ), the absorption is generally predicted by the phonon-assisted transition and impurity effect in  $\text{In}_2\text{O}_3$ . The plots of logarithm of absorption coefficient ( $\ln\alpha$ ) as a function of photon energy ( $\hbar\omega$ ) for  $\text{In}_2\text{O}_3$  and of mixed oxides  $\text{In}_2\text{O}_3$ - $\text{MoO}_3$  system are shown in Figs 1c-4c. The values of  $E_c$  are estimated and listed in the Tables I-IV. The plots of ( $\ln\alpha$ ) versus ( $\hbar\omega$ ) for thickness, substrate temperature and annealing of mixed oxides  $\text{In}_2\text{O}_3$ - $\text{MoO}_3$  system are not shown in the text, but for comparison the values of  $E_c$  are estimated and listed in the Tables V-VII.

Electron diffraction studies demonstrate that freshly evaporated films of  $\text{In}_2\text{O}_3$  and of mixed oxides  $\text{In}_2\text{O}_3$ - $\text{MoO}_3$  system deposited in vacuum on a substrate at room temperature are effectively amorphous in structure. The  $\text{In}_2\text{O}_3$  films prepared on a substrate at a temperature of  $270^\circ\text{C}$  are amorphous in character where as the films of mixed oxides  $\text{In}_2\text{O}_3$ - $\text{MoO}_3$  system prepared on a substrate at a temperature of  $270^\circ\text{C}$  are polycrystalline. On annealing in vacuum the films become crystalline and many of the defects associated with the films are annealed out. The comparison of the values of Urbach energy  $E_c$  and

TABLE VII Effect of annealing temperature on some optical parameters of amorphous thin films of fixed composition (85 mol.%  $\text{In}_2\text{O}_3$ -15 mol.%  $\text{MoO}_3$ ) having thickness  $\approx 300$  nm deposited at  $20^\circ\text{C}$

Annealing temperature ( $^\circ\text{C}$ )	$E_{\text{opt}}$ (eV)	$E_c$ (eV)
As evaporated	2.15	0.95
200	1.63	1.00
300	1.32	1.15
400	0.70	1.18
500	0.65	1.19

optical band gap  $E_{\text{opt}}$  of  $\text{In}_2\text{O}_3$  and of mixed oxides system  $\text{In}_2\text{O}_3$ - $\text{MoO}_3$  is carried out and results are discussed. The values of film thickness, optical band gap and other parameters are estimated very accurately and are listed in the Tables I-VII.

#### 4. Discussion

In general, the preparation of evaporated dielectric films introduces extrinsic centres, which contribute to changes in the optical properties. These centres can arise from the presence of impurities introduced during preparation and by contamination when the samples were exposed to air. Such defects, together with structural defects (e.g. voids), are assumed to give rise to localized states in the band gap.

Indium can exist with valencies of two or three. The valency state in which it most commonly occurs is In(III). Under normal conditions  $\text{In}_2\text{O}_3$  crystallizes in the C-type rare earth structure, which is very stable [27]. In  $\text{In}_2\text{O}_3$  every fourth anion is missing so that small anion sites constitute interstitial sites in the oxygen sub-lattice. The energy of formation of oxygen interstitials in the C-type structure should be small. If the energy of migration is also small, these interstitials will be mobile and oxygen diffusion via interstitials will result, thus primary ionic defects will be oxygen ion vacancies and indium interstitials. It has been proposed by Klein [28] that the conduction band in  $\text{In}_2\text{O}_3$  arises mainly from 5s electrons and the valence band is from oxygen 2p electrons. The Fermi energy  $E_f$  in the pure material lies halfway between energy band edges. Kiriakidis *et al.* [29] have observed the non-stoichiometric nature of vacuum deposited films and reported that this non-stoichiometric nature is probably due to the oxygen vacancies or metal excess. Ramaiah *et al.* [8] have suggested that amorphous films deposited at room temperature have a slight excess of indium over the stoichiometric composition and conduction electrons in  $\text{In}_2\text{O}_3$  arise from the excess indium atoms.

It is well known that  $\text{MoO}_3$  loses oxygen on heating in vacuum or in reducing atmosphere and our amorphous layers are thus assumed to be deficient in oxygen.  $\text{MoO}_3$  has the outer electron configuration  $4s^5 5s^1$ . If  $\text{MoO}_3$  is considered to be ionic i.e. composed only of Mo(VI) and  $\text{O}^{-2}$  ions, the valence band would be composed of oxygen 2p states and the conduction band of

empty 4d<sup>0</sup> and 5s states [30]. The electronic configuration of Mo(VI) is 4d<sup>0</sup>, so the transition from the valence 2p oxygen orbitals to empty Mo(VI) 4d<sup>0</sup> levels gives rise to the incorporation of lower valence Mo(V) within the lattice. Sub-stoichiometric amorphous thin films of MoO<sub>3</sub> contain a number of oxygen ion vacancies (donor centres) which are positively charged structural defects capable of capturing one or two electrons and into which electrons may be promoted. These donor centres exist in the forbidden gap of the insulator and form a defect band below the conduction band [31, 32].

In the present work the optical absorption spectra of amorphous thin films of In<sub>2</sub>O<sub>3</sub> have been studied in the thickness range 100–400 nm with the substrate at room temperature during deposition. Some samples have been studied in the substrate deposition temperature range 20–270°C. Some samples of mixed oxides system In<sub>2</sub>O<sub>3</sub>–MoO<sub>3</sub> have been studied at constant thickness approximately 300 nm but of different compositions (different molar percentage). Some samples of In<sub>2</sub>O<sub>3</sub>–MoO<sub>3</sub> have been studied at fixed composition but different thicknesses in the range 100–400 nm and different substrate deposition temperatures in the range 20–270°C. A few samples of In<sub>2</sub>O<sub>3</sub> and of mixed oxides In<sub>2</sub>O<sub>3</sub>–MoO<sub>3</sub> system were annealed in the temperature range 200–500°C for 4 h.

The results of optical absorption spectra mentioned in this work show the following main points

1. In case of pure In<sub>2</sub>O<sub>3</sub> samples, the optical band gap is decreased with increase in film thickness, substrate deposition temperature and annealing (Tables I–III).
2. In case of mixed oxides In<sub>2</sub>O<sub>3</sub>–MoO<sub>3</sub> system, the optical band gap is also decreased as the molar fraction of MoO<sub>3</sub> is increased in In<sub>2</sub>O<sub>3</sub> films at constant film thickness. A decrease in the band gap of mixed oxides In<sub>2</sub>O<sub>3</sub>–MoO<sub>3</sub> system of fixed composition with film thickness, substrate deposition temperature and annealing has also been observed (Tables IV–VII).
3. It has also been demonstrated that in mixed oxides In<sub>2</sub>O<sub>3</sub>–MoO<sub>3</sub> system the optical band gap is much smaller than for the pure In<sub>2</sub>O<sub>3</sub> thin films.

The observed results are explained as follows:

When the thickness of In<sub>2</sub>O<sub>3</sub> amorphous thin films is increased, the concentration of oxygen vacancies, i.e. positively charged structural defects, is increased due to thermal evaporation of In<sub>2</sub>O<sub>3</sub> in vacuum. Thus initially when the thickness is increased, oxygen vacancies generate carriers in the films. The degree of localization of electrons increases with the increase in cation concentration thereby increasing the number of donor centres. A large concentration of donor centres, effectively lowers the band gap and shifts the absorption edge to the higher wavelength region.

Kim *et al.* [33] have suggested that films of In<sub>2</sub>O<sub>3</sub> prepared on substrates at a temperature of 270°C or higher

are crystalline, but the present investigation showed that In<sub>2</sub>O<sub>3</sub> films prepared on substrates at a temperature of 270°C are amorphous in character. These conflicts are most likely due to their different methods of film growth. Since the properties of the films depend strongly on the structure, stoichiometry and nature of the impurities present, it is inevitable that each deposition technique with its associated controlling parameters should yield films with different characteristics.

In In<sub>2</sub>O<sub>3</sub> two kinds of ionic defects are produced at higher substrate temperature, namely, oxygen vacancies and indium interstitials (In<sub>i</sub>) [34]. Ohta *et al.* [3] have suggested the movement of In<sub>i</sub> (indium interstitial) defects while measuring the oxidation state of indium metal at higher temperatures. The decrease in optical energy due to an increase in substrate temperature is ascribed to the release of trapped electrons by thermal energy or by the outward diffusion of the oxygen-ion vacancies, which are quite mobile even at low temperature. As the substrate temperature is increased, less interstitial oxygen and more oxygen vacancies and indium interstitials are incorporated in the oxide. At higher substrate temperature oxygen vacancies act as doubly ionized donors and contribute two electrons as charge carriers due to which optical band gap is decreased.

Electron diffraction studies revealed that after annealing the samples at 500°C most of the defects are annealed out and a crystalline state is established. Our films were annealed with a heater wound around a mica frame. Oxygen was supposed to be incorporated in the films by degassing from the mica sheet during heating. Kiriakidis *et al.* [29] have reported that the concentration of oxygen vacancies decreases as oxygen enters in the lattices of indium. Since oxygen was absorbed as O<sub>2</sub> molecules in the lattices of indium, the concentration of oxygen vacancies is reduced which may deteriorate the film properties and consequently reduce the mobility of the carriers. The decrease in band gap may be due either to the increasing concentration of these types of defects or to the formation of indium species of lower oxidation state (In<sup>2+</sup>).

Molybdenum can exist with valencies of four, five and six. The valency state in which it most commonly occurs is Mo(VI). When the molar percentage of MoO<sub>3</sub> is increased in the mixed layers of In<sub>2</sub>O<sub>3</sub>–MoO<sub>3</sub>, there is an increase in the over all disorder in the system. Mo(VI) ions are incorporated in an In<sub>2</sub>O<sub>3</sub> lattice causing the indium orbital to become a little less tightly bound. The presence of Mo(VI) ions in an In<sub>2</sub>O<sub>3</sub> lattice have caused a decrease in the optical band gap. Optical band gap is also decreased with increase in film thickness of the samples having fixed composition (85 mol.% In<sub>2</sub>O<sub>3</sub>–15 mol.% MoO<sub>3</sub>). When the thickness of the samples is increased, the concentration of oxygen vacancies is increased in In<sub>2</sub>O<sub>3</sub> and MoO<sub>3</sub> thin films. The incorporation of Mo(VI) ions in an In<sub>2</sub>O<sub>3</sub> lattice may also enhance the electron concentration but the oxygen vacancies are believed to be the source of conduction electron states in In<sub>2</sub>O<sub>3</sub>–MoO<sub>3</sub> complex.

The optical band gap is decreased with the increase in substrate deposition temperature of the mixed oxides films of constant thickness and fixed composition (85 mol.%  $\text{In}_2\text{O}_3$ –15 mol.%  $\text{MoO}_3$ ) having thickness approximately 300 nm. The decrease in optical band gap with increasing substrate temperature is due to increasing concentration of  $\text{In}_i$  defects and to the formation of indium and molybdenum species of lower oxidation states.

When substrate temperature is increased, the colour of the mixed oxides  $\text{In}_2\text{O}_3$ – $\text{MoO}_3$  samples is changed from white to blue. The reduction in band gap in the samples is due to the centres formed by capturing an electron in doubly charged oxygen vacancy whose level lies close to the valence band. The blue coloured films exhibit a small band near the Fermi level. This band is attributed to the electrons trapped in positively charged anion vacancies within the film structure. The blue colour is caused by the inter-electron transfer from oxygen 2p to molybdenum 4d orbital that creates the isolated Mo(V) species of lower oxidation state.

The decrease in optical band gap of (85 mol.%  $\text{In}_2\text{O}_3$ –15 mol.%  $\text{MoO}_3$ ) samples of thickness 300 nm due to increase in annealing temperature may result due to three reasons. (i) Reduction in the concentration of lattice imperfections due to annealing the samples in vacuum. At higher annealing temperature upto 500°C or above most of the defects are annealed out and a crystalline state is established. (ii) Two types of defects are produced in  $\text{In}_2\text{O}_3$  at higher temperature, namely, oxygen vacancies and indium interstitials. (iii) Indium and molybdenum species of lower oxidation states are formed at higher annealing temperature, so that In(III) centres may change to In(II) and Mo (VI) centres may change to Mo(IV) valency states.

Thus decrease in band gap due to annealing the mixed oxides  $\text{In}_2\text{O}_3$ – $\text{MoO}_3$  samples is attributed to the formation of Mo and In species of lower oxidation states, increasing concentration of oxygen vacancies, indium interstitials and reduction in lattice imperfections.

## 5. Conclusion

On the basis of the above-mentioned observations, it is concluded that decrease in optical band gap with increase in thickness of  $\text{In}_2\text{O}_3$  thin films is ascribed to the concentration of oxygen vacancies, which are incorporated in the film structure during vacuum evaporation. The changes associated with the increase in substrate temperature are due to increase in oxygen vacancies and indium interstitials. The changes with increase in annealing temperature are due to the formation of indium species of lower oxidation state or to a decrease in the concentration of lattice imperfections. When  $\text{MoO}_3$  is incorporated in  $\text{In}_2\text{O}_3$ , some Mo(VI) ions are introduced in  $\text{In}_2\text{O}_3$  lattice that causes the indium orbital to become a little less tightly bound. As a consequence the optical band gap is decreased. The

decrease in band gap due to increase in substrate temperature and annealing the mixed oxides  $\text{In}_2\text{O}_3$ – $\text{MoO}_3$  samples is attributed to the formation of Mo and In species of lower oxidation states, increasing concentration of oxygen vacancies, indium interstitials and reduction in lattice imperfections. The blue colouration of the samples is due to the formation of Mo species of lower oxidation state that are formed by the inter-electron transfer from oxygen 2p to the molybdenum 4d level.

## References

1. H. L. HARTNAGEL, A. L. DAWAR, A. K. JAIN and C. JAGADISH, "Semiconducting Transparent Thin Films" (Institute of Physics, Bristol, 1995).
2. Y. SHIGESATO and D. C. PAINE, *Thin Solid Films*, **238** (1994) 44.
3. H. OHTA, M. ORITA, M. HIRANO and H. HOSONO, *J. Appl. Phys.* **91** (6) (2002) 3547.
4. G. B. GONZALIZ, J. B. COHEN, J. H. HWANG, T. O. MASON, J. P. HODGES and J. D. JORGENSEN, *ibid.* **89** (2001) 2550.
5. M. GIRTAN and G. I. RUSU, *Fizica Starri Condensate*, **XLV-XLVI** (1999) 166.
6. K. ARSHAK and K. TWOMEY, *Sensors*, **2** (2002) 205.
7. D. D. EDWARDS, T. O. MASON, F. GOUTENOIRE and K. R. POEPELMEIER, *Appl. Phys. Lett.* **70** (13) (1997) 1706.
8. K. S. RAMAIAH, V. S. RAJA, A. K. BHATNAGAR, R. D. TOMLINSON, R. D. PILKINGTON, A. E. HILL, S. J. CHANG, Y. K. SU and F. S. JUANG, *Semicond. Sci. Technol.* **15** (7) (2000) 676.
9. P. MANIVANNAN and A. SUBRAHMANYAM, *J. Phys. D: Appl. Phys.* **27** (1993) 1085.
10. J. ASBALTER and A. SUBRAHMANYAM, *J. Vac. Sci. and Technol.* **18** (1999) 1672.
11. D. MANNO, M. DI GIULIO, A. SERRA, T. SICILIANO and G. MICOCCI, *J. Phys. D: Appl. Phys.* **35** (2002) 228.
12. T. MARUYAMA and T. KANAGAWA, *J. Electrochem. Soc.* **142** (1995) 1644.
13. M. CHEN, U. V. WAGHMARE, C. M. FRIEND and E. KAXIRAS, *J. Chem. Phys.* **109** (1998) 6854.
14. J. ZHOU, S. Z. DENG, N. S. XU, J. CHEN, and J. C. SHE, *Appl. Phys. Letts.* **83** (2003) 2653.
15. WANG CHENGYU and H. U. YINGJIE, *J. Chinese Ceramic Soc.* **24**(5) (1996) 654.
16. M. KHARRAZI, L. KULLMAN and C. G. GRANQVIST, *Solar Energy Materials and Solar Cells.* **53** (1998) 349.
17. T. IVANOVA, A. SZEKERES, M. GARTNER, D. GOGOVA and K. A. GESHEVA, *Electrochimica Acta.* **46** (2001) 2215.
18. Y. ZHAO, J. LIN, Y. ZHOU, Z. ZHANG, Y. XU, H. NARAMATO and S. YAMAMOTO, *J. Phys: Conden. Matter.* **15** (2003) L547.
19. A. SIOKOU, G. LEFTHERIOTIS, S. PAPAETHIMIOU and P. YIANOULIS, *Surf. Sci.* **482** (2001) 294.
20. M. YAHYA, M. M. SALLEH, I. A. TALIB and M. M. NOR, Third International Conference on Thin Film Physics and Application Shanghai, China, *SPIE Proc.* (1998) 42.
21. K. V. MADHURI, K. S. RAO, S. UTHANNA, B. S. NAIDU and O. M. HUSSAIN, *J. Indian Inst. Sec.* **81** (2001) 653.
22. M. ANWAR, I. M. GHOURI and S. A. SIDDIQI, *Czech. J. Phys.* **55**(8) (2005) 1013.
23. J. TAUC, R. GRIGOROVICI and A. VANCU, *Phys. Stat. Sol.* **15** (1966) 627.
24. E. A. DAVIS and N. F. MOTT, *Phil. Mag.* **22** (1970) 903.
25. S. K. J. AL-ANI and A. A. HIGAZY, *J. Mater. Sci.* **26** (1991) 3670.
26. F. URBACH, *Phys. Rev.* **92** (1953) 1324.
27. C. GOEBBERT, R. NONNINGER, M. A. AEGERTER and H. SCHMIDT, *Thin Solid Films*, **351** (1999) 79.



28. A. KLEIN, *Appl. Phys. Lett.* **77** (2000) 2009.
29. G. KIRIAKIDIS, H. OUACHA and N. KATSARAKIS, *Rev. Adv. Mater. Sci.* **4** (2003) 32.
30. S. A. BUKESOV, J. Y. KIM, A. V. STRELTSON and D. Y. JEON, *J. Appl. Phys.* **91** (11) (2002) 9078.
31. M. M. BAGHERI-MOHAGHEGHI and M. SHOKOOAH-SAREMI, *Semicond. Sci. Technol.* **18** (1997) 103.
32. A. TAURINO, M. CATALANO, R. RELLA, P. SICILIANO and W. WLODARSKI, *J. Appl. Phys.* **93** (7) (2003) 3816.
33. H. KIM, C. M. GILMORE, A. PIQUE, J. S. HORWITZ, H. MATTOUSSI, H. MURATA, Z. H. KAFABI, and D. B. CHRISEY, *ibid.* **86** (1999) 6451.
34. M. ANWAR, I. M. GHOURI, and S. A. SIDDIQI, Electronic Conductions in  $\text{In}_2\text{O}_3$ , *Czech J. Phys.* **55**(10) (2005) 1261.

*Received 28 June  
and accepted 7 July 2005*